

FORMATION, COOLING HISTORY AND AGE OF IMPACTS ON THE IIE IRON PARENT BODY: EVIDENCE FROM THE MILES METEORITE. Rachel S. Kirby¹, Penelope L. King¹, Marc D. Norman¹, Trevor R. Ireland¹, Margaret Forster¹, Arthur D. Pelton², Ulrike Troitzsch¹, Nobumichi Tamura³ and Michael L. Turner⁴
¹Research School of Earth Sciences, The Australian National University (ANU), Acton ACT 2601, Australia, ²Center for Research in Computational Thermochemistry, Department of Chemical Engineering, Polytechnique Montréal, Montréal QC H3T 1J4 Canada, ³Advanced Light Source, Lawrence Berkeley National Laboratory, 1 Cyclotron Road, Berkeley, CA 94720, U.S.A. ⁴Research School of Physics and Engineering, ANU, Acton ACT 2601, Australia.

Introduction: Most iron meteorites formed in planetary cores during differentiation; however, IIE iron meteorites have chemical and physical features that are inconsistent with this origin [e.g. 1]. Furthermore, IIE irons are a texturally and compositionally diverse group with variable ratios of metal to silicate inclusions, a range of peak temperatures (T) and low pressure (P) recorded in their chemistry and mineralogy, inclusion compositions that range from chondritic through mafic and felsic, and metal textures that imply a range of cooling rates and equilibrium temperatures [e.g. 2-4]. Ages obtained for IIE iron meteorites cluster into two groups: ~4.5Ga and ~3.6 Ga [e.g. 5]. Any petrogenetic model for the IIE iron meteorites must explain formation of chondritic and felsic inclusion(s) at a range of peak T and low P at ~25 Myr after solar system formation followed by a range of cooling rates. We demonstrate that these features are most consistent with multiple impact heating events on a porous planetesimal, most likely the H chondrite parent body [3, 6].

Methods: The Miles IIE iron meteorite was analyzed for this study as its mineralogy indicates high temperatures and an old age, thus it likely preserves evidence of the formation conditions of the IIE iron meteorites. A detailed methodology is in [3].

Petrogenetic Context: Petrography of the Miles meteorite is consistent with solidification from an immiscible Fe-Ni and silicate melt [4]. Synchrotron micro-scanning X-ray diffraction found disordered srilankite constraining $T \geq 1160^\circ\text{C}$ [7] and tridymite indicating $P < 0.7$ GPa [3]. Rapid cooling is evidenced by the disordered srilankite, lack of Widmanstätten pattern [8] and thermodynamic modelling suggesting Scheil-Gulliver cooling prevailed [3]. The $f\text{O}_2$ was 1.43 to 2.09 log units below the iron-wüstite buffer from coexisting ferropseudobrookite, rutile and metal [9].

The petrogenesis of the silicate inclusions in Miles is revealed from their major element chemistry determined by scanning electron microscopy energy dispersive spectroscopy. Inclusions grouped from felsic to intermediate produce a sequence in composition similar to that observed when synthesized H chondrite material undergoes increasing degrees of partial melting

(increasing T) at low-P and low $f\text{O}_2$ conditions [10]. This is consistent with Miles forming at the high T end of the IIE iron meteorite spectrum, with felsic inclusions crystallizing from H chondrite partial melts. At the other end of the spectrum, IIE iron meteorites with chondritic inclusions (e.g. Netschaëvo) formed at lower T than those with felsic inclusions [920-1080°C; 11]. Petrography of the inclusions, including the presence of relict chondrules, suggests they are chondritic xenoliths and not crystallized partial melts.

Miles has a $^{207}\text{Pb}/^{206}\text{Pb}$ age of 4542 Ma [4], therefore the high temperatures determined for the mineral assemblage require a significant energy source 25 Ma after the formation of the solar system, followed by rapid cooling. Impacts into porous targets may provide sufficient thermal energy for heating and even result in localized melting [12] at times when short-lived radionuclides had become extinct.

In Miles, we found $^{39}\text{Ar}/^{40}\text{Ar}$ ages of 4.3 Ga and 3.5 Ga [3], with both dates in agreement with those reported in other IIE iron meteorites [5]. This is the first IIE iron meteorite found to record events both early in the solar system and during the Late Heavy Bombardment, revealing a complex petrogenetic and thermal history of Miles and the IIE iron meteorites.

A range of cooling rates across the group is also inferred from the range of metallographic textures, with some IIE irons containing Widmanstätten textures (e.g. Garhi Yasin) [13].

Petrogenesis of the IIE iron meteorites: Combining these geochemical, petrologic and mineralogic studies with physical and thermodynamic modelling we suggest the IIE iron meteorites have a common history (Fig. 1). At 4542 Ma the iron-rich, porous parent body was impacted. Higher porosity regions experienced higher peak temperatures, resulting in localized melting forming a series of melt lenses and dikes. These melts immediately began to cool as heat escaped from the body, with the cooling rate depending on the depth of burial within the impact structure and the size of the melt lens or dike. Within melt lenses and dikes, immiscible metallic iron and silicate liquids underwent density separation that segregated metallic iron which percolated down through fractures forming

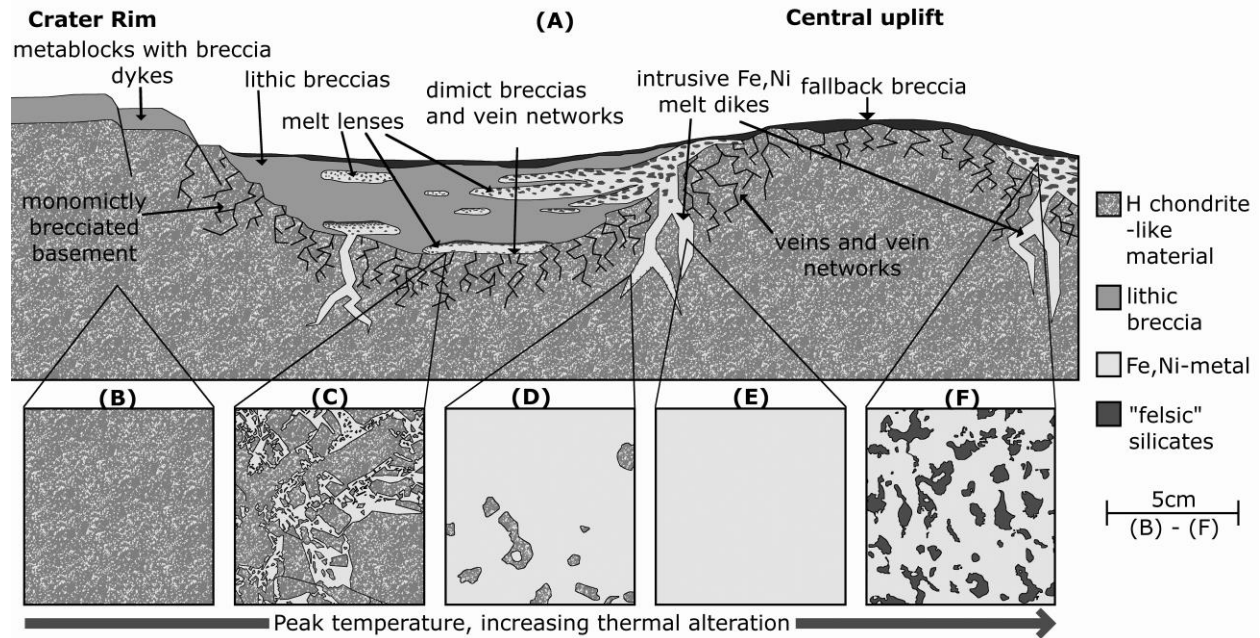


Figure 1: Schematic cross-section of part of the impact crater with melt lenses and dikes that formed the IIE irons and related meteorites. B-F: (boxes are 5cm across) examples of the textures that formed in various regions of the impact crater/melt pool shown in cross-section. B: unaltered H chondrite parent body, e.g. Hamburg H4 chondrite. C: Dimict breccia of H chondrite clasts within metal veins, e.g. Portales Valley H chondrite. D: metal with altered H chondrite-like and mafic clasts, e.g. Netschaëvo, Watson 001, Techado, Roberts Massif 04186 and Mont Dieu. E: Silicate-free IIE metal, e.g. Arlington and Barranca Blanca. F: metal with recrystallized felsic silicates, e.g. Miles, Wekeroo Station, Colomera, Kodaikanal, Elga, Tarahumara and Taylor Glacier 05181. In general, the peak temperature experienced during the impact event and the subsequent thermal alteration increases from B to F. Note, a central uplift will only form if the crater is sufficiently large.

metal veins surrounding angular chondritic clasts, e.g., Portales Valley H chondrite.

Heat transferred from melt lenses into the surrounding chondritic material resulted in high T partial melting, forming felsic melts enriched in incompatible elements. Rapid cooling of the metallic melts trapped some of these felsic silicate melts as inclusions in the metal before full separation could occur (e.g. Miles).

IIE iron meteorites with mafic and chondritic inclusions such as Netschaëvo likely formed at lower T at the margins of dikes. Here, clasts of chondritic parent body material became entrained within the partially crystalline metal, forming relatively unmodified to thermally metamorphosed angular xenoliths.

Large silicate-free masses of Fe-Ni metal underwent slower cooling, allowing for gravity separation of silicates and Widmansätten pattern formed in metal (e.g., Arlington [13]), likely in the center of large melt lenses and dikes. The body was impacted again at ~3.6 Ga with a range of cooling rates.

Conclusions: The IIE irons formed during an impact event 4542 Ma, with peak temperatures and cooling rates dependent on their proximity to the impact

site, parent body porosity, and capacity to transfer heat away during cooling. These meteorites sample lenses, dikes and parent body material in and around the impact structure in which each experienced a different thermal history, resulting in a wide variety of chemical and mineralogical features amongst the group whilst maintaining a similar siderophile element composition in the metal. Oxygen isotopes and siderophile element composition of the metal suggests that these meteorites formed on the H chondrite parent body [3, 6].

References: [1] Ruzicka A. (2014) *Chemie der Erde*, 74, 3-48. [2] Wasson J.T. (2017) *GCA*, 197,396-416. [3] Kirby R.S. et al. (Under Review) *GCA*. [4] Kirby R.S. et al. (2016) *LPS XLVII*, #1903. [5] Bogard D.D. et al. (2000) *GCA*, 64, 2133-2154. [6] Kirby R.S. et al. (2022) *LPS LIII*. [7] Troitzsch U. and Ellis D.J. (2005) *J. Mater. Sci.*, 40, 4571-4577. [8] Ikeda Y. et al. (1997). *Antarctic Meteor. Res.*, 10, 355-372. [9] Simons B. and Woermann E. (1978), *Contrib. Mineral. Petrol.*, 66, 81-89. [10] Collinet M. and Grove T.L. (2020) *GCA*, 277, 334-357. [11] Van Roosbroek et al. (2015) *Meteoritics & Planet. Sci.*, 50, 1-13. [12] Bland P.A. et al. (2014) *Nat. Commun.*, 5, 1-13. [13] Buchwald V.F. (1975) *Handbook of Iron Meteorites*.